The Astrophysical Journal, 816:65 (16pp), 2016 January 10 doi:10.3847/0004-637X/816/2/65

BLACK HOLE MERGERS AND BLUE STRAGGLERS FROM HIERARCHICAL TRIPLES FORMED IN GLOBULAR CLUSTERS

Fabio Antonini, Sourav Chatterjee, Carl L. Rodriguez, Meagan Morscher, Bharath Pattabiraman, Vicky Kalogera, and Frederic A. Rasio
Center for Interdisciplinary Exploration and Research in Astrophysics (CIERA) and Department of Physics and Astrophysics, Northwestern University, Evanston, IL 60208, USA
Received 2015 September 14; accepted 2015 October 30; published 2016 January 8

ABSTRACT

Hierarchical triple-star systems are expected to form frequently via close binary–binary encounters in the dense cores of globular clusters (GCs). In a sufficiently inclined triple, gravitational interactions between the inner and outer binary can cause large-amplitude oscillations in the eccentricity of the inner orbit ("Lidov–Kozai (LK) cycles"), which can lead to a collision and merger of the two inner components. In this paper we use Monte Carlo models of dense star clusters to identify all triple systems formed dynamically and we compute their evolution using a highly accurate three-body integrator which incorporates relativistic and tidal effects. We find that a large fraction of these triples evolve through a non-secular dynamical phase which can drive the inner binary to higher eccentricities than predicted by the standard secular perturbation theory (even including octupole-order terms). We place constraints on the importance of LK-induced mergers for producing: (i) gravitational wave sources detectable by Advanced LIGO (aLIGO), for triples with an inner pair of stellar black holes (BHs); and (ii) blue straggler stars, for triples with main-sequence-star components. We find a realistic aLIGO detection rate of BH mergers due to the LK mechanism of $\sim 1\ \mathrm{yr}^{-1}$, with about 20% of these having a finite eccentricity when they first chirp into the aLIGO frequency band. While rare, these events are likely to dominate among eccentric compact object inspirals that are potentially detectable by aLIGO. For blue stragglers, we find that the LK mechanism can contribute up to $\sim$10% of their total numbers in GCs.

Key words: blue stragglers – galaxies: star clusters: general – gravitational waves

1. INTRODUCTION

Observations indicate that a large fraction of stars reside in triple systems (Riddle et al. 2015, and references therein). In a dynamically stable non-coplanar triple the gravitational interaction between the inner and outer binary drives periodic/quasi-periodic variations of the mutual inclination between the two orbits and of the eccentricity of the inner binary (Lidov 1961; Kozai 1962). Such eccentricity oscillations, first discovered by Lidov (1961), can lead to a close approach between the inner binary components, which can produce a variety of exotic astrophysical phenomena, including compact-object and stellar binary mergers (e.g., Miller & Hamilton 2002; Ford et al. 2004; Antonini et al. 2010; Naoz & Fabrycky 2014), X-ray binaries, SN Ia and gamma-ray bursts (Thompson 2011; Hamers et al. 2013).

Lidov–Kozai (LK) oscillations are usually described as a secular phenomenon, occurring on timescales much longer than the orbital period of the outer binary orbit (e.g., Ford et al. 2004; Fabrycky & Tremaine 2007; Naoz et al. 2013). The standard approach is to make use of the so-called orbit-averaging technique in which one computes the mutual gravitational interaction (torques) between two mass weighted ellipses instead of point masses on orbits. The basic assumption is that the evolution of the orbital parameters occurs on a timescale much longer than the dynamical timescales of the system (e.g., Merritt 2013).

The orbit averaged equations of motion can describe the evolution of a wide range of systems, but become inaccurate once the triple hierarchy is moderate. Antonini & Perets (2012) showed that the orbit-average treatment, even at the octupole level of approximation, becomes inaccurate in hierarchical systems where the tertiary comes closer to the inner binary than a certain distance. At the high eccentricity phase of a LK cycle the timescale for the angular momentum perturbation due to the tertiary can become comparable to or shorter than the dynamical timescales of the system, rendering the secular approach no longer valid (Antonini & Perets 2012; Katz & Dong 2012; Seto 2013; Antognini et al. 2014; Antonini et al. 2014; Bode & Wegg 2014). In this case, the binary can be driven to a much closer separation than the secular theory would otherwise predict. This can have important consequences for the evolution of the inner binary. For example, Antonini & Perets (2012), Seto (2013), and Antonini et al. (2014) demonstrated that in this non-secular regime, a compact object binary can be pushed inside the 10 Hz gravitational wave (GW) frequency band of Advanced Ligo (aLIGO) detectors with a finite eccentricity. Similarly, in the case of stellar binaries, the two stars could be driven to a direct collision. Naoz & Fabrycky (2014) and Perets (2015) suggested that direct stellar collisions driven by the LK mechanism might have an important role in the formation of blue straggler stars (BSSs) in stellar clusters.

Globular clusters (GCs) are a natural environment for forming triples and higher order multiples. On one hand, the dense stellar environment of GCs is hostile to triples. In fact, given the high densities of GCs, triples may be involved in close encounters which tend to destroy them. On the other hand, the high stellar densities that characterize the core of GCs favor dynamical binary–binary interactions that naturally lead to the formation of stable triples (Sigurdsson & Hernquist 1993), including black hole (BH) triples and mixed, compact object-star, triples that could not otherwise form. The inner binaries in the triples may be driven to merge before their next interaction. Interestingly, such mergers have been

suggested early on as a channel for the formation of compact-object mergers (Miller & Hamilton 2002; Wen 2003; Arca-Sedda 2016), and more recently as a channel for the formation of BSSs through mass transfer and mergers (Perets & Fabrycky 2009; Leigh & Sills 2011; Geller et al. 2013; Naoz & Fabrycky 2014; Perets 2015).

In this paper we study the evolution of dynamically assembled triples inside GCs, with particular focus on triples containing an inner main-sequence (MS) stellar binary and triples with an inner BH binary. We do not consider here the evolution of mixed star-compact object systems, or binaries containing evolved (e.g., red giant) stars; we reserve a study of these latter systems to a future investigation. In this paper we use a Monte Carlo code to simulate the long-term evolution of GCs (Morscher et al. 2015), and identify all triple systems formed during the cluster evolution. We then evolved these triples using a high-accuracy direct three-body integrator which includes tidal and general relativity (GR) effects for both the inner and outer orbit. Scattering with other stars is also accounted for, but only in the sense that the triples are evolved for a time equal to the timescale over which they will be disrupted through gravitational encounters with other stars. The results of the direct integrations are used to determine the rate of BH and stellar binary mergers induced by the LK mechanism in GCs.

Although previous studies have shown that triples can form quite frequently in GCs, their detailed long-term dynamical evolution in the cluster environment has not been yet investigated. Our study sheds light on exactly this point, i.e., it allows us to assess for the first time the role of the host cluster evolution and its properties on the formation and dynamics of the triples. This allows us to place reliable constraints on the contribution of mergers from triples to BSS populations and on the event rate and properties of inspiraling BH binaries as a source of GW radiation for aLIGO detectors (e.g., Aasi et al. 2015; Acernese et al. 2015).

We note that the dynamics of triples with either an inner stellar or compact object component has been investigated by many authors and in a variety of contexts (including stellar triples, planets around stars, supermassive BH mergers), using the standard orbit averaged formalism and therefore fully neglecting non-secular effects (e.g., Blaes et al. 2002; Wen 2003; Naoz et al. 2011, 2013; Hamers et al. 2013; Naoz & Fabrycky 2014). The new ingredients of our study, compared to previous work dealing with similar problems, are: (i) the use of realistic initial conditions for our triple populations that were directly obtained using Monte Carlo models of the long-term dynamical evolution of GCs; (ii) the use of accurate three-body integrations that allow an essentially exact treatment of the triple dynamics, avoiding the approximations that are made when using the secular equations of motion.

The paper is organized as follows. We begin with a discussion of dynamically assembled triples in GCs and their properties in Section 2, and show that for most triples the orbit average approximation is expected to break down. In Section 3 we discuss our GC models, triple initial conditions, and adopted numerical methods. We present our results on BH-triples and associated aLIGO event rates in Section 4. In Section 5 we describe the results concerning stellar triples and their implications for BSS formation in GCs. We further discuss the implications of our results in Section 6. Section 7 provides a summary.

2. BREAK-DOWN OF THE SECULAR APPROXIMATION

We consider a binary of components of masses m_0 and m_1 orbiting a third body of mass m_2. We indicate the eccentricities of the inner and outer orbits, respectively, as e_1 and e_2, and semimajor axes a_1 and a_2; we define ω_1 as the argument of periapsis of the inner binary relative to the line of the descending node, ω_2 as the argument of periapsis of the outer orbit, and I as the orbital inclination of the inner orbit relative to the outer orbit.

In what follows we only consider triple systems that satisfy the stability criterion of Mardling & Aarseth (2001),

$$\frac{a_2}{a_1} > \frac{3.3}{1-e_2}\left[\frac{2}{3}\left(1+\frac{m_2}{M_b}\right)\frac{1+e_2}{(1-e_2)^{1/2}}\right]^{2/5} \times (1-0.3I/\pi), \quad (1)$$

with $M_b = m_0 + m_1$.

If the system satisfies the stability criterion (1) it is also reasonable to describe the dynamics of the entire system as the interaction between an inner binary of point masses m_0 and m_1 and an external binary of masses M_b and m_2. We define the angular momenta L_1 and L_2 of the inner and outer binary:

$$L_1 = m_0 m_1 \left[\frac{G a_1 \left(1-e_1^2\right)}{M_b}\right]^{1/2}, \quad (2)$$

and

$$L_2 = M_b\ m_2 \left[\frac{G a_2 \left(1-e_2^2\right)}{M_b + m_2}\right]^{1/2}, \quad (3)$$

with G the gravitational constant. The dimensionless angular momenta are $\ell_1 = L_1/L_{1,c}$ and $\ell_2 = L_2/L_{2,c}$, with $L_{i,c} = L_i/\sqrt{1-e_i^2}$ as the angular momentum of a circular orbit with the same semimajor axis, a_i.

If the changes in the orbital properties of the inner binary caused by its gravitational interaction with the third body occur on a timescale longer than both the inner binary orbital period, P_1, and the tertiary orbital period, P_2, it is convenient to average the equations of motion over the rapidly varying mean anomalies of the inner and outer orbits (e.g., Hamers et al. 2015). The resulting double averaged Hamiltonian is $\mathcal{H} = kW$ with $k = 3Gm_0m_1m_2a_1^2/[8M_b a_2^3(1-e_2^2)^{3/2}]$ and (Lidov & Ziglin 1976; Miller & Hamilton 2002)

$$W(\omega_1, e_1) = -2\left(1-e_1^2\right) + (1-e_1^2)\cos^2 I + 5e_1^2 \sin^2\omega_1(\cos^2 I - 1). \quad (4)$$

The quadrupole-level secular perturbation equations can be easily derived from the conserved Hamiltonian (4). The resulting evolution equation of the inner binary orbital angular momentum due to the torque from the tertiary is (e.g., Lidov & Ziglin 1976):

$$\frac{d\ell_1}{dt} = -\frac{15\pi}{4}\frac{m_2}{M_b}\frac{a_1^3}{a_2^3\left(1-e_2^2\right)^{3/2}}\frac{e_1^2}{P_1}\sin^2 I \sin 2\omega_1. \quad (5)$$

The characteristic timescale for the eccentricity oscillations is (Holman et al. 1997):

$$T_{\rm LK} \simeq P_1 \left(\frac{M_b}{m_2}\right)\left(\frac{a_2}{a_1}\right)^3 \left(1-e_2^2\right)^{3/2}. \quad (6)$$

Using Equation (5) and taking the relevant limit $e_1 \to 1$, we find that the maximal change in the inner binary angular momentum due to the interaction with the third object and over the inner binary orbital period is

$$\delta \ell_{\rm in} \approx 4\pi \frac{m_2}{M_b} \frac{a_1^3}{a_2^3\left(1-e_2^2\right)^{3/2}}, \quad (7)$$

and the change in the binary angular momentum over one orbit of the tertiary is

$$\delta \ell_{\rm out} \approx \delta \ell_{\rm in} \frac{P_2}{P_1}; \quad (8)$$

thus, the change experienced over the timescale associated with the period of the outer orbit is naturally P_2/P_1 larger than the change experienced over the inner binary orbital period.

Equation (4) describes the gravitational interaction of two weighted ellipses rather than point masses on orbits and is accurate as long as $\delta \ell_{\rm out}/\ell_1 \lesssim 1$, i.e., changes of the inner binary angular momentum occur on a timescale longer than the tertiary orbital period. If instead the change in the inner binary angular momentum over the inner and outer orbital periods is of order ℓ_1, then the system no longer meets the conditions required for the orbit averaged approximation, and more accurate direct three-body integrations are needed.

Following the discussion above, in order to address the reliability of the orbit averaged approach in describing the evolution of a triple system it is useful to compare the change in angular momentum of the binary to the critical angular momentum $\ell_{\rm diss} \approx \sqrt{2 D_{\rm diss}/a_1}$, where $D_{\rm diss}$ is the scale at which other dynamical processes will dominate the evolution of the inner binary. Since in this paper we focus on triples in which the inner binary can be driven to a strong close interaction or even a merger, we identify these processes with energy loss due to GW radiation and tidal dissipation in the case of BH and stellar binaries, respectively.

The condition that the inner binary undergoes rapid eccentricity oscillations over the *outer* orbital period can be written as $q_{\rm out} \equiv \delta \ell_{\rm out}/\ell_{\rm diss} \gtrsim 1$; this requirement translates into a condition on the outer perturber separation,

$$\frac{a_2}{a_1} \lesssim \frac{3}{1-e_2^2}\left(\frac{m_2}{M_b}\right)^{2/3}\left(\frac{M_b}{M_b+m_2}\right)^{1/3}\left(\frac{a_1}{D_{\rm diss}}\right)^{1/3}. \quad (9)$$

We call this regime "moderately" non-secular. In this regime systems can experience eccentricity oscillations over the outer binary period and can be driven to higher eccentricities than secular theory would otherwise predict, which in the case of compact object binaries could result in substantially reduced merger times (Antognini et al. 2014).

If $q_{\rm in} \equiv \delta \ell_{\rm in}/\ell_{\rm diss} \gtrsim 1$, the inner binary will undergo eccentricity oscillations on the timescale of the *inner* orbital period; this can be achieved if the tertiary comes closer to the inner binary than the separation

$$\frac{a_2}{a_1} \lesssim \frac{2.5}{1-e_2}\left(\frac{m_2}{M_b}\right)^{1/3}\left(\frac{a_1}{D_{\rm diss}}\right)^{1/6}. \quad (10)$$

We call the regime defined by this equation "strongly" non-secular (see also Antonini & Perets 2012 and Equation (7) in Katz & Dong 2012). In this situation the outer perturber is close enough to significantly change the angular momentum of the eccentric binary at the last apoapsis passage leading to a jump in angular momentum of order ℓ_1. The angular momentum of an eccentric inner binary can jump from several times $\ell_{\rm diss}$ (far enough to avoid GR or tidal effects) to an arbitrarily small value. Equation (10) defines the region of parameter space within which a compact object binary might be expected to enter the aLIGO frequency band with a finite eccentricity (Antonini & Perets 2012; Seto 2013; Antonini et al. 2014) or, in the case of inner stellar components, the binary members might experience a close interaction leading to a stellar collision (Katz & Dong 2012; Prodan et al. 2015).

Here we quantify the role of non-secular effects for triple systems forming in stellar clusters by analyzing the properties of all dynamically stable triples that were produced in the GC Monte Carlo models of Morscher et al. (2015) (see Section 3.2). The Monte Carlo models give the masses, stellar radii, semimajor axes, eccentricities, and stellar type of all triples formed during the cluster dynamical evolution; these properties were used to make Figure 1, which shows the period distributions as well as the distribution of the ratio $a_2(1-e_2)/a_1$ of all BH triples (left panels) and stellar triples (right panels) that formed in these models.[1]

In Figure 1 we have distinguished triples which satisfied the criterion (9) (green histograms) and those meeting the more stringent condition Equation (10) (blue histograms) from the remaining systems which satisfied neither conditions. In the case of stellar triples we evaluated Equations (9) and (10) setting $D_{\rm diss} = 2(R_0 + R_1)$ with R_0 and R_1 the physical radii of the inner binary components (Katz & Dong 2012), while for BH triples we adopted a conservative dissipation scale of $D_{\rm diss} = 10^9$ cm (Antonini et al. 2014).

Figure 1 shows that for the majority of BH triples formed non-secular dynamical effects are expected to become important before GR terms can significantly affect the evolution of the inner binary. We conclude that the standard LK secular theory will fail in describing the evolution of these systems due to the breakdown of the double averaging approximation.

Only a few stellar triples in our sample satisfy condition (10), mainly because of their large value of $D_{\rm diss}$. However, a large fraction of stellar triples still met the condition Equation (9), meaning that the averaging procedure over the outer orbit is not justified for many of these systems.

In what follows we study the dynamical evolution of triples that form through dynamical interactions in the dense stellar environment of GCs. We use a high accuracy three-body integrator to study how the inner binary in the triples might evolve to become a possible source of GW radiation for aLIGO detectors, or, in the case of stellar binaries, how the evolution might lead to a mass transfer event or even a stellar merger. We begin in the next section by describing the initial conditions and numerical methods adopted in our study.

[1] Hereafter we define as a stellar triple any stable triple in which both components of the inner binary are MS stars; BH triples are identified with triples in which the two inner components are both stellar BHs.

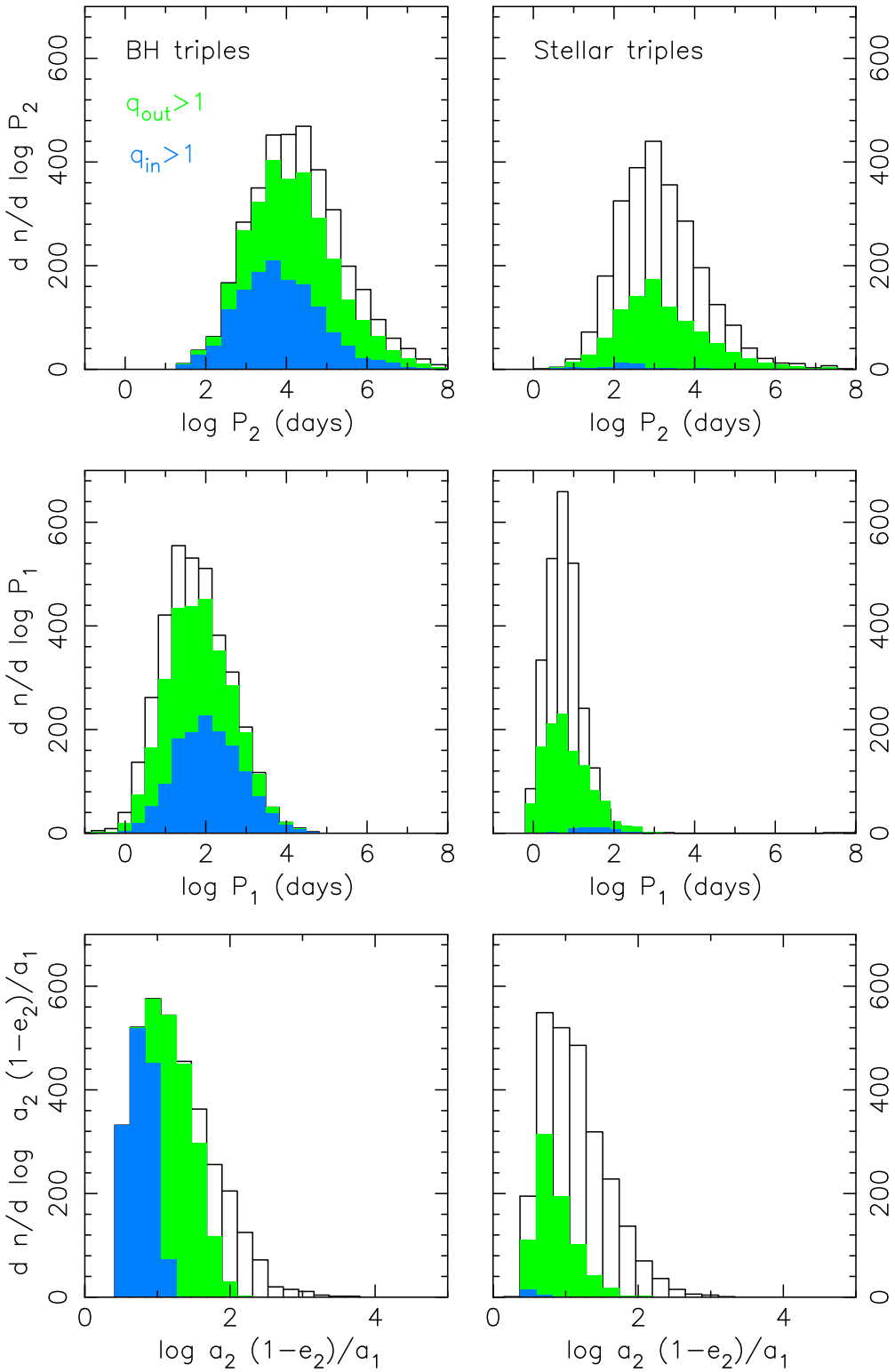

Figure 1. The upper and middle panels show the distribution of inner and outer orbital periods of the BH and stellar triples formed in the Monte Carlo models of Morscher et al. (2015). The bottom panel gives the distribution of the ratio between the outer binary periapsis and inner binary semimajor axis. The blue and green histograms indicate systems for which the assumptions on which the orbit averaged approximation is based on break down before GR or tides can affect their evolution. The green histograms are systems for which $q_{\rm out} \equiv \delta\ell_{\rm out}/\ell_{\rm diss} \gtrsim 1$; the blue histograms are systems for which $q_{\rm in} \equiv \delta\ell_{\rm in}/\ell_{\rm diss} \gtrsim 1$. For many triples formed through dynamical interactions in star clusters, the secular approximation breaks down well above their typical dissipation scale, and the LK equations of motion (even at the octupole order level) cannot accurately trace the evolution of these systems.

3. METHODS AND INITIAL CONDITIONS

3.1. Numerical Methods and Example Cases

The direct three-body integrations presented below were performed using the ARCHAIN integrator (Mikkola & Merritt 2008). ARCHAIN employs an algorithmically regularized chain structure and the time-transformed leapfrog scheme to accurately integrate the motion of arbitrarily tight binaries with arbitrarily large mass-ratio. The code also includes post-Newtonian (PN) non-dissipative 1PN, 2PN, and dissipative 2.5PN corrections to all pair-forces. We refer the reader to Mikkola & Merritt (2008) for a more detailed description of ARCHAIN. We also used the octupole level secular equations of motion given in Blaes et al. (2002) to evolve the systems, which allowed us to directly compare the predictions of the direct integrations to the orbit averaged results.

In the case of triples containing an inner stellar binary (stellar triples), to the PN terms we also added terms that account for dissipative tides as well as apsidal precession induced by tidal bulges. In order to do so we modified ARCHAIN, including terms to the equations of motion that represent tidal friction and quadrupolar distortion. Velocity-dependent forces were included via the generalized mid-point method described in Mikkola & Merritt (2006); this method allows us to time-symmetrize the algorithmic regularization leapfrog even when the forces depend on velocities, permitting the efficient use of extrapolation methods. The tidal perturbation force has the form

$$\boldsymbol{F} = -G\frac{m_0 m_1}{r^2}\left\{3\frac{m_0}{m_1}\left(\frac{R_1}{r}\right)^5 k\left(1+3\frac{\dot{r}}{r}\tau\right)\hat{r}\right\}, \qquad (11)$$

where τ (here set to a fixed value of 1 s) is the time lag, and k (set to 0.03) is the apsidal motion constant.

Equation (11) differs from the classical treatment of near-equilibrium tides to the extent that we have suppressed terms that are due to the difference in rotation rate between the binary and each component. The orbital elements evolution equations that correspond to Equation (11) are given by Equations (9) and (10) of Hut (1981); these standard equations were implemented in the secular integrations to account for dissipative as well as non-dissipative tides.

To illustrate the importance of non-secular effects for the dynamics of the systems under consideration, we show two examples in Figure 2. We consider a BH triple that is in the strongly non-secular regime defined by Equation (10), as well as a stellar triple that is in the moderately non-secular regime defined by Equation (9). The evolution of the two systems was computed using both the secular equations of motion and ARCHAIN.

The examples of Figure 2 demonstrate how the double-orbit-averaging procedure can lead to misleading results when applied to the dynamics of systems that evolve to attain very high orbital eccentricities. In the upper panel the three-body integration predicts that the inner binary will merge within a few LK oscillations, whereas the secular calculation predicts that the system does not merge in the considered time interval. More importantly, in the direct three-body integration the binary was found to have a substantial eccentricity of $e_1 \approx 5 \times 10^{-2}$ at the moment its peak GW frequency (Equation (13) below) reached 10 Hz. In the lower panel the stellar binary also attains higher eccentricities when integrated with ARCHAIN, which might induce a mass transfer event or reduce the circularization time due to tidal friction when compared to the secular integrations.

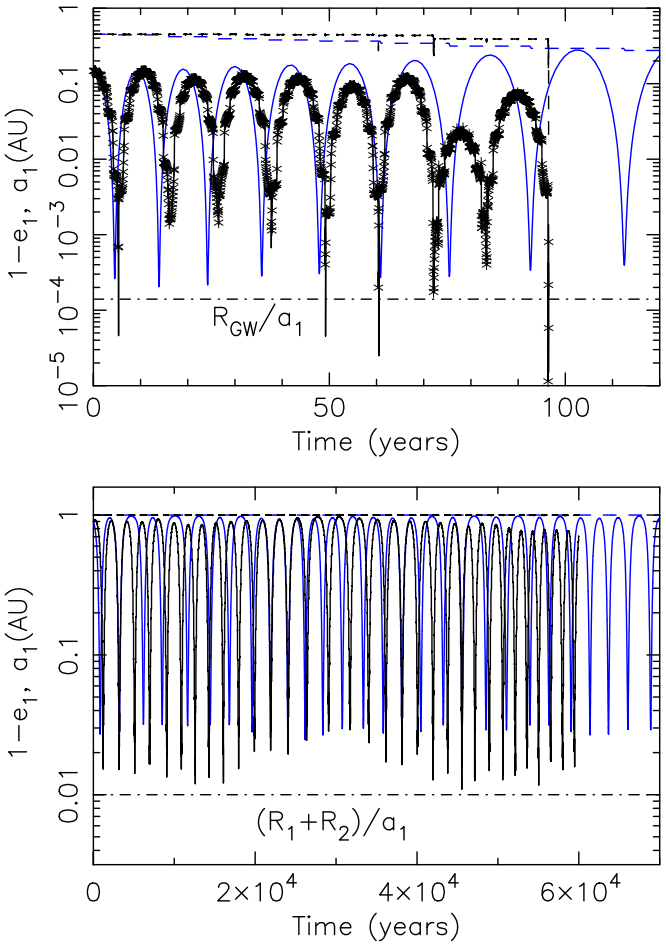

Figure 2. Dynamical evolution of a BH triple (upper panel) and a stellar triple (lower panel). Black lines show the results of three-body integrations, blue lines show the results of the octupole order orbit averaged equations of motion. Solid lines give the value of $(1 - e_1)$, and dashed lines give the inner binary semimajor axis. In the upper panel the initial conditions for the BH triple system were: $m_0 = 14.9\ M_\odot$, $m_1 = 13.8\ M_\odot$, $m_2 = 14.2\ M_\odot$ $a_1 = 0.45$ AU, $a_2 = 3.9$ AU, $e_1 = 0.85$, $e_2 = 0.51$, $I = 92.^\circ5$, $\omega_1 = \omega_2 = \pi/2$. In the lower panel the initial conditions for the stellar triple were: $m_0 = 0.7\ M_\odot$, $m_1 = 0.5\ M_\odot$, $m_2 = 2\ M_\odot$ $a_1 = 1$ AU, $a_2 = 25$ AU, $I = 101.^\circ8$, $e_1 = 0.1$, $e_2 = 0.7$, $\omega_1 = 214.^\circ6$, $\omega_2 = 0$. In the upper panel the asterisks denote the minimum separation attained by the two BHs every orbital period. At $(1 - e_1) \lesssim 10^{-3}$ this system satisfies the condition $q_{\rm in} \gtrsim 1$, so that the jump in periapsis over one inner orbit is of the order of the periapsis distance itself. In the lower panel at $(1 - e_1) \lesssim 0.04$ the triple satisfies the condition $q_{\rm out} \gtrsim 1$, so that the averaging procedure over the outer orbit is no longer justified. In both examples the inner binary reaches higher eccentricities in the three-body simulation than in the secular integration. This allows the two BHs in the upper panel to merge through GW energy loss, and the two stars in the lower panel to approach each other close enough that mass transfer would commence. The dotted–dashed lines indicate the critical value of $(1 - e_1)$, below which GW radiation will dominate (upper panel), and below which the two stars will collide (lower panel). These two examples clearly illustrate the limitation of the standard secular approach even when including octupole order terms to the equations of motion.

3.2. GC Models and Initial Conditions

The initial conditions for the triple systems used in this analysis were taken from the Monte Carlo simulations of Morscher et al. (2015). This study presents 42 Monte Carlo dynamical simulations of massive star clusters containing large

populations of stellar BHs. The Monte Carlo technique simulates two-body relaxation in the Fokker–Planck approximation through representative pair-wise scattering interactions (Hénon 1971; Chatterjee et al. 2010).

Our implementation in the Cluster Monte Carlo (CMC) code (Pattabiraman et al. 2013, and references therein) includes direct integration of strong three- and four-body (binary–single and binary–binary) encounters, direct physical collisions, single and interacting binary stellar evolution, and tidal interactions with the Galaxy. Primordial triples are not included in these models. However, during strong binary–binary interactions, it is possible to form stable hierarchical triple systems (Rasio et al. 1995). Limitations in CMC currently require that these triples be broken artificially at the end of the timestep. Nonetheless, whenever a stable triple is formed, its properties are logged, including the masses, radii, and star types for the stellar components, and the semimajor axes and eccentricities for the inner and outer orbits. Since we lack information regarding the mutual orientation of the two orbits, we sample $\omega_{1(2)}$ and $\cos(I)$ randomly from a uniform distribution with $65^\circ \leqslant I \leqslant 115^\circ$. The initial orbital phases in the three-body integrations were also randomly distributed.

We extracted the properties for every stable triple system formed through dynamical interactions over 12 Gyr across all of the 42 models presented in Morscher et al. (2015), and from five additional models provided by the same authors (M. Morscher 2015, private communication). The main properties of the 47 cluster models are reported in Rodriguez et al. (2015); these span a large range of masses (from $2 \times 10^5\,M_\odot$ to $1.6 \times 10^6\,M_\odot$), of virial radii (from 0.5 to 4 pc), and metallicities ($Z = 0.0005$, 0.0001 and 0.005). We note that, because these triple systems are destroyed in the Monte Carlo simulation, it is possible for the components of these triples to subsequently form new triple systems, when in reality they could in principle survive for a significant period of time.

In the high-density stellar environment of GCs, triples may be perturbed through encounters with other passing stars on timescales that can be shorter than the relevant LK timescale. Such encounters will alter the orbital properties of the triple significantly, or even disrupt it. To account for this we set the final integration time in our simulations equal to the encounter timescale for collisions with other stars (Binney & Tremaine 1987; Ivanova et al. 2008),

$$T_{\rm enc} \approx 8.5 \times 10^{12}\ {\rm years}\ P_2^{-4/3} M_{\rm tri}^{-2/3} \sigma_{10}^{-1} n_5^{-1} \times \left[1 + 913 \frac{M_{\rm tri} + \langle M \rangle}{2 P_2^{2/3} M_{\rm tri}^{1/3} \sigma_{10}^2}\right]^{-1}, \quad (12)$$

where σ_{10} is the central velocity dispersion of the cluster in units of 10 km s^{-1}, $M_{\rm tri} = M_b + m_2$ is the mass of the triple, $\langle M \rangle$ is the mass of an average star in the cluster, and n_5 is the local number density of stars in units of 10^5 pc^{-3}. The values of n, $\langle M \rangle$ and σ in Equation (12) were obtained directly from the Monte Carlo models and correspond to to their values in the cluster core at the moment the triple system was formed. We then integrate each triple until a time $T_{\rm enc}$ was reached, or until the inner binary had merged.

In total, the Monte Carlo models contain 8864 triples. Of these 5238 are BH triples; 3626 have at least one non-BH component in the inner binary, and of these, in the inner binary, 2940 have two MS stars, 260 have a BH plus another MS star, 218 have a white dwarf plus another MS star, 4 have a neutron star (NS) plus a MS star, 163 have a MS star plus an evolved star (red giant or later type), and 2 have a BH plus an evolved star. The remaining systems include 32 triples with an inner white dwarf binary, 5 triples with an inner BH plus white dwarf binary, and 2 triples with an inner BH plus NS binary. No triple with an inner NS binary is seen in any of these Monte Carlo models. Of the 5238 BH triples, 3852 satisfy the condition $T_{\rm LK} \geqslant T_{\rm enc}$, whereas 2519 of the 2940 stellar triples with an inner MS binary satisfied this condition.

4. RESULTS: BH TRIPLES

For each of the 3852 BH triples extracted from the Monte Carlo models we made 10 realizations, each adopting a random orientation of the two orbits and random orbital phases. Of the total 38,520 BH triples that we evolved with ARCHAIN, 2080 resulted in a merger of the two inner BHs. The total number of BH mergers obtained when using the orbit averaged equations of motion was 1796 instead. We found that the merger time of such binaries after the triple was formed was typically very short and always shorter than $\lesssim 10^5$ years. Thus, the BH mergers discussed in what follows will occur inside the GCs even when the recoil velocity at formation can be large enough to eject the triple from the cluster core. In this section we discuss the properties of the merging compact binaries, including their eccentricity, mass, merger time distribution, and event rates.

Eccentric binaries emit a GW signal with a broad spectrum of frequencies. The peak GW frequency associated with the harmonic that leads to the maximal emission of GW radiation can be estimated as (Wen 2003)

$$f_{\rm GW} = \frac{\sqrt{G M_b}}{\pi} \frac{\left(1 + e_1\right)^{1.1954}}{\left[a_1\left(1 - e_1^2\right)\right]^{1.5}}. \quad (13)$$

We approximately follow the time evolution of the GW frequency of the inner BH binaries through Equation (13). This allowed us to estimate the eccentricity of the BH binary when its GW frequency is $\gtrsim$10 Hz, i.e., when it would be large enough to be into the aLIGO frequency band (Abadie et al. 2010).

Figure 3 gives the ratio of the triple survival timescale, $T_{\rm enc}$, to the LK timescale plotted against the value of $a_2(1 - e_2)/a_1$. From this plot we see that non-secular dynamical effects are expected to become important to the evolution of most BH triples in our models, possibly leading to the formation of eccentric GW sources. Also, most BH mergers are found to occur in moderately hierarchical triples with $a_2(1 - e_2)/a_1 \lesssim 10$. This is expected for at least two reasons: (1) the closer the outer body to the inner binary the less significant is the quenching of the LK cycles due to relativistic precession of the inner binary (e.g., Blaes et al. 2002), so that typically the smaller the ratio $a_2(1 - e_2)/a_1$ the larger the maximum eccentricity attained by the inner binary, and consequently, the shorter its merger time; (2) triples with a small $a_2(1 - e_2)/a_1$ ratio, also have a larger $T_{\rm enc}/T_{\rm LK}$ ratio, which naturally leads to a higher chance for a merger before the triple is disrupted by gravitational encounters with other stars. In Figure 3 we also identify those systems for which at least 1 of the 10 random realizations led to a merger (blue points) and those for which at least 1 realization produced a BH binary

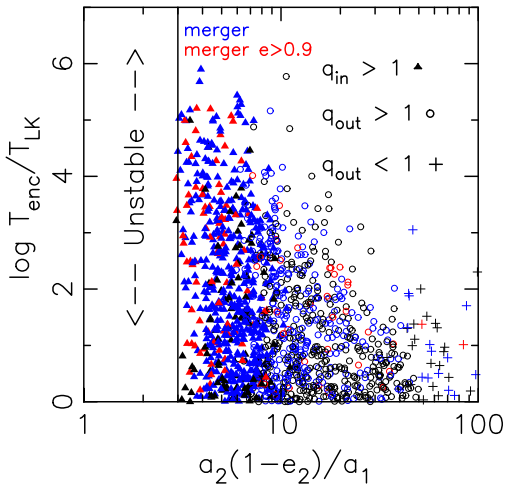

Figure 3. Ratio of the triple survival time in the GC core to the LK timescale as a function of the ratio $a_2(1-e_2)/a_1$. Triangle symbols represent systems that satisfy the condition Equation (10), open circles are systems which satisfy the condition Equation (9) but not the condition Equation (10) and plus symbols are systems which satisfy neither of these two conditions. We evolved each of these systems 10 times, selecting randomly the initial inclination as detailed in the text. Blue colored points are systems in which in at least of the 10 realizations we found one merger within T_{enc}. Red points are systems in which for at least one of the ten realizations the inner binary eccentricity was larger than 0.9 at the moment its peak GW frequency became larger than 10 Hz. As predicted, most eccentric mergers occur in triples for which the orbit averaging over the inner binary breaks down.

merger with an eccentricity larger than 0.9 at $\gtrsim$10 Hz frequency (red symbols). As predicted on the basis of our discussion in Section 2, most eccentric mergers occur at $a_2(1-e_2)/a_1 \lesssim 10$, near the boundary for instability.

Figure 4 shows the eccentricity distribution of all BH binary mergers in our simulations, when the associated f_{GW} *first* enters the 10 and 40 Hz frequency bands. Figures 5 and 6 show the corresponding merger time and mass distribution of the merging binaries. The distributions shown in Figures 4–6 were obtained by weighing the number of mergers for each cluster model by the likelihood of that model to represent a typical GC in the Milky Way (MW). More in detail, the weights are obtained by creating a kernel density estimate (W_{MW}) of the MW GCs on the fundamental plane (which we take to be mass and ratio of the half to core radius), then estimating the weight for each model using the kernel density estimate at the position of that model on the fundamental plane. In this way, cluster models that are more likely to be drawn from the same distribution of MW GCs are more heavily weighted. The weight for a model of total mass M_{GC}, core radius R_c and half mass radius R_h after 12 Gyr of evolution is computed as:

$$W\left(M,\, R_c\,/R_h\right) = \frac{W_{MW}\left(M,\, R_c/R_h\right)}{W_{Models}\left(M,\, R_c/R_h\right)}, \qquad (14)$$

where we have divided by W_{Models}, the kernel density estimate of the models themselves. This serves to normalize the distribution, so that regions of parameter space that are over-sampled by the models are given lower weights (see Rodriguez et al. 2015, for more details). The fraction of mergers with a given property (e.g., total mass, eccentricity) is then simply $f = \sum_i N_i W_i / \sum_i W_i$, with N_i as the number of mergers occurring in the i_{th} cluster model.

Huerta & Brown (2013) showed that for eccentricities less than $e_1 \lesssim 0.1$ at $\approx$10 Hz, circular templates will be effective at recovering the GW signal of eccentric sources. Figure 4 shows that approximately 20% of all BH mergers in our three-body integrations had an eccentricity $e > 0.1$ at $\gtrsim$10 Hz frequency. This percentage drops to $\sim$10% at 40 Hz frequency. The difference with the results of the secular equations of motion is evident in these plots. The secular integrations clearly underestimate the number of eccentric mergers producing just a few percent of inspirals with $e \gtrsim 0.1$ at 10 Hz frequency. The direct three-body integrations also produce a significant population ($\sim$15% of the total) of highly eccentric sources in the aLIGO frequency window, which are fully missed when evolving the triples with the secular equations of motion. These sources will start to inspiral due to GW radiation energy loss within the aLIGO band with an extremely high eccentricity, $1 - e_1 \lesssim 10^{-4}$, and a characteristic GW frequency. In fact, the angular momentum of BH binaries that evolve into the strongly non secular regime can be arbitrarily small at the moment energy loss due to GW radiation starts to become dominant. For this reason the GW frequency at which the binary enters the aLIGO band, which depends on the binary angular momentum via Equation (13), could be significantly larger than 10 Hz. (see the example of Figure 3 in Antonini et al. 2014). We note that the detectability of such sources also depends on how much energy is radiated around 100 Hz where aLIGO is more sensitive. So it is important to see at what frequency these sources first enter the aLIGO sensitivity window. Based on our simulations we found that all eccentric BH binaries will enter the aLIGO band at $\lesssim$300 Hz and 80% of them had $f_{GW} < 50$ Hz when they first entered the aLIGO frequency band (see also Figure 7 in Antonini et al. 2014). We conclude that most eccentric sources could be detected by aLIGO, provided that an efficient search strategy is used.

Figure 5 displays the average merger time distribution of BH binaries induced by the LK mechanism in our models. The figure shows a clear peak around 1 Gyr of evolution with a long tail extending to the present epoch. The declining merger rate is mostly due to the decreasing total number of BHs in our models with time. As the rate depends on the total number of BHs in the cluster core it drops with time as BHs are continuously ejected from the cluster through strong dynamical interactions.

Figure 6 displays the chirp mass, $M_{ch} = (m_0 m_1)^{3/5}/(m_0 + m_1)^{1/5}$, as well as the total mass distribution of the merging BH binaries. These distributions appear to be consistent with that of dynamically formed binaries shown in Figure 2 of Rodriguez et al. (2015). Figure 6 shows a mass distribution peaked around $M_{ch} \approx 17\ M_\odot$, while the highest chirp mass of BH binaries formed by pure stellar evolution over all our models was $\approx$13 $M_\odot$. This latter value for the chirp mass is the maximum for primordial binaries in our GC simulations that evolved without significant dynamical encounters (see also Downing et al. 2010; Rodriguez et al. 2015). The fact that the typical chirp mass of the merging BH binaries in Figure 6 is substantially larger than $\approx$13 $M_\odot$ is a result of the naturally stronger segregation of the heaviest BHs as well as the preferential ejection of the lightest BHs from the clusters during dynamical interactions. As the heavier BHs segregate more efficiently to the cluster center and the lighter BHs are ejected through binary single interactions, the former will tend to dominate the cluster core, where binary–binary interactions

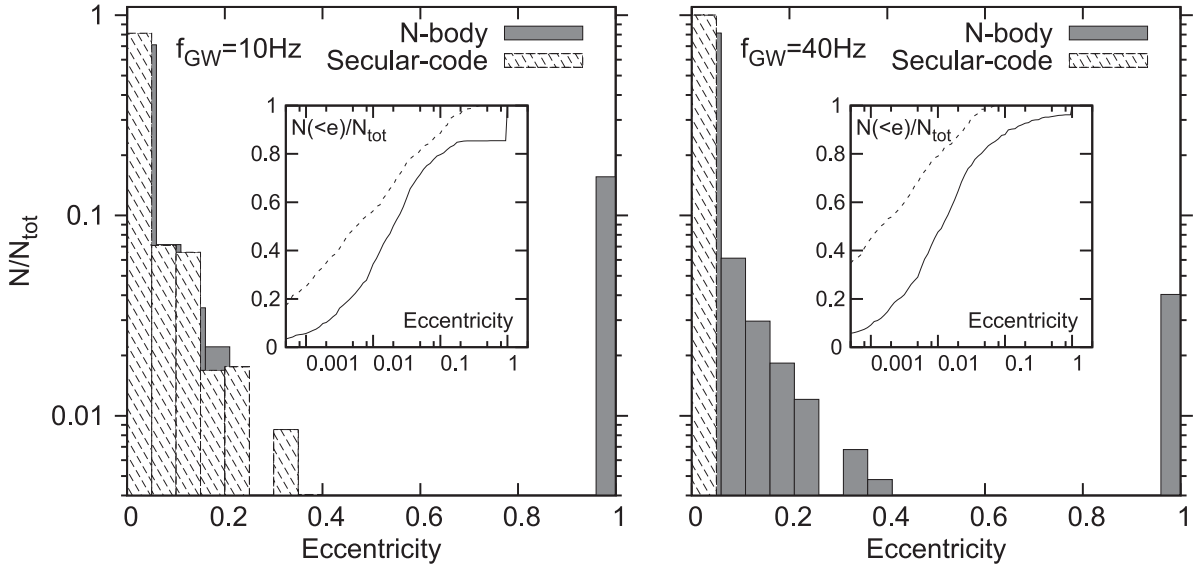

Figure 4. Eccentricity distribution of merging BH binaries at the moment they first enter the 10 Hz (left panel) and 40 Hz (right panel) frequency bands. While the *octupole* level secular equation of motions predict that only a few percent of systems will have finite eccentricity as they enter the aLIGO band, accurate *N*-body integrations show that ∼20% (∼10%) of BH mergers in GC will have an eccentricity larger than 0.1 at 10 Hz (40 Hz) frequency. About 10% (∼5%) of all mergers will have extremely high eccentricities, i.e., $1 - e \lesssim 10^{-4}$, at 10 Hz (40 Hz) frequency. Note that the stippled regions are in front in both panels, which means that the lack of stippled regions at high eccentricities is because there are none, rather than because they are hidden behind the solid hystograms.

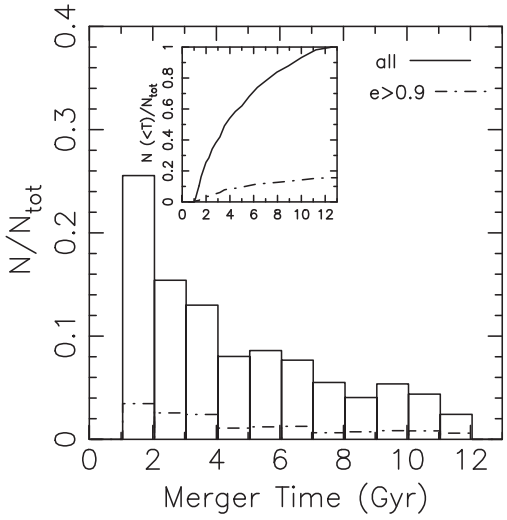

Figure 5. Merger time distribution of BH binaries due to the LK mechanism in GCs. Continious lines give the merger time distribution of all BH binary mergers, and the dashed line is for BH binaries that have $e > 0.9$ when $f_{\rm GW} \geqslant 10$ Hz. The inset panel gives the corresponding cumulative distributions.

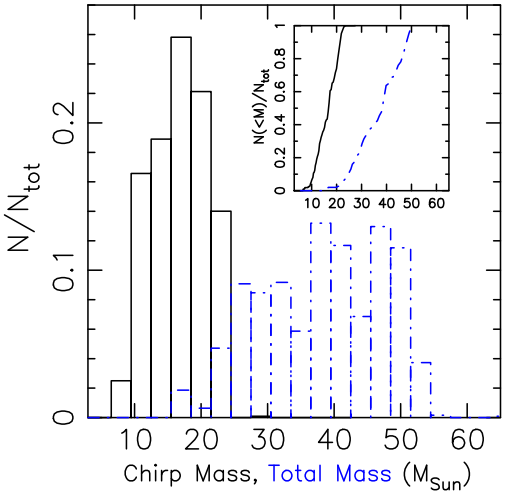

Figure 6. Continuous black lines show the chirp mass distribution of BH binary mergers due to the LK mechanism in GCs. Dot–dashed blue lines give the distribution of total mass for the merging binaries. The inset panel gives the corresponding cumulative distributions.

can lead to the formation of stable BH triples and to LK induced mergers.

4.1. BH Merger Detection Rate

One of the advantages of using realistic CMC models is that it allows us to make direct predictions about the mass and merger time distribution of the coalescing BH binaries, which is fundamental to make reliable estimates for the event and detection rates. As we have complete information about the distribution of sources in time and chirp mass, we can compare our ensemble of GC models to observations of MW and extragalactic GCs and estimate the merger rate for a single aLIGO detector.

To compute the rate of detectable sources per year from triple systems, we follow a similar procedure to Rodriguez et al. (2015). The rate is expressed as the following double integral over source chirp mass and redshift:

$$R_d = \iint \mathcal{R}(\mathcal{M}_{\rm c}, z) f_d(\mathcal{M}_{\rm c}, z) \frac{dV_{\rm c}}{dz} \frac{dt_s}{dt_0} d\mathcal{M}_{\rm c} dz, \qquad (15)$$

where

1. $\mathcal{R}(\mathcal{M}_{\rm c}, z)$ is the rate of BH binary mergers with chirp mass $\mathcal{M}_{\rm c}$ at redshift z due to the LK mechanism.
2. $f_d(\mathcal{M}_{\rm c}, z)$ is the fraction of sources with chirp mass $\mathcal{M}_{\rm c}$ at redshift z that are detectable by a single aLIGO detector.
3. $dV_{\rm c}/dz$ is the comoving volume at a given redshift (Hogg 1999). We assume cosmological parameters of

$\Omega_M = 0.309$, $\Omega_\Lambda = 0.691$, and $h = 0.677$, from the combined Planck results (Planck Collaboration et al. 2015).

4. $dt_s/dt_0 = 1/(1+z)$ is the time dilation between a clock measuring the merger rate at the source versus a clock on Earth.

The rate is expressed as the product of the mean number of triple sources per GC, the distribution of sources in $\mathcal{M}_c$–z space, and the spatial density of GCs per Mpc^3 in the local universe (0.77 Mpc^{-3}, from Rodriguez et al. 2015, Supplemental Materials). Symbolically, this becomes $\mathcal{R}(\mathcal{M}_c, z) = \langle N \rangle \times P(\mathcal{M}_c, z) \times \rho_{GC}$.

The components of $\mathcal{R}(\mathcal{M}_c, z)$ are computed as follows. The mean number of sources per GC is found by performing a weighted linear regression between the number of triple mergers a GC produces over its lifetime, and the final mass of the GC at 12 Gyr. The number of triple mergers for a given cluster is obtained by multiplying the total number of mergers obtained from the three-body integrations by a factor $\cos(65^\circ) \times 0.1$; where the first term takes into account the fact that we have only considered inclinations $65^\circ \leqslant I \leqslant 115^\circ$ and the second term takes into account the fact that for each triple we have performed 10 integrations with random orbital orientations and phases. The weights are assigned using $W_{MW}(M, R_c/R_h)$, the numerator from Equation (14). This linear regression is then multiplied by a universal GC luminosity function (Harris et al. 2014), and integrated over mass (assuming a mass-to-light ratio of 2) to yield a mean number of sources. This average is then multiplied by the distribution of sources, found by randomly drawing a number of mergers from each model according to the weights in Equation (14), then generating a kernel density estimate of these sources in chirp mass/redshift space. Note that unlike Rodriguez et al. (2015), we do not separately consider the populations of low-metallicity and high-metallicity GCs.

Finally, we model the efficiency of an aLIGO detector by calculating the fraction of sources at chirp mass $\mathcal{M}_c$ and redshift z that aLIGO could detect, marginalized over all possible sky locations and binary orientations. We use IMRPhenomC waveforms (Santamaría et al. 2010) and the projected zero-detuning, high-power aLIGO noise curve.[2] Note that this template family does *not* consider the eccentricity of sources, which could dramatically alter the gravitational waveforms (Huerta & Brown 2013). Such simplification does not significantly alter the total detection rate estimates presented here; in fact, our simulations show that at 10 Hz frequency ∼80% of coalescing BH binaries have an eccentricity $e_1 \lesssim 0.1$, which is small enough that circular templates will be efficient at recovering their GW signal (Brown & Zimmerman 2010; Huerta & Brown 2013).

As $P(\mathcal{M}_c, z)$ is dependent on the random draw of mergers, we report the mean of R_d over 100 separate draws. We also provide optimistic and pessimistic rate estimates to approximate the uncertainties associated with our assumptions. The optimistic rates are computed by assuming the $+1\sigma$ value of the 100 draws of R_d, the $+1\sigma$ uncertainty for the linear regression between GC mass and number of mergers, a highly optimistic upper limit on the GC mass function ($2 \times 10^8\, M_\odot$), and the upper-limit on ρ_{GC} of 2.3 Mpc^{-3} from Rodriguez et al. (2015). Conversely, the pessimistic rate estimate assumes the corresponding -1σ uncertainties, a pessimistic upper limit on the GC mass function ($4 \times 10^6\, M_\odot$), and the lower-limit of ρ_{GC} of 0.32 Mpc^{-3}.

For all LK driven events, we find that a single aLIGO detector could detect ∼0.5 events per year (pessimistically ∼0.1 yr^{-1}, optimistically ∼2 yr^{-1}).

We performed the same analysis described above for all eccentric sources produced in our three-body simulations, i.e., we computed the detection rate solely for eccentric systems assuming perfect templates for detecting eccentric binaries. Thus, the results of this computation *do not* represent the number of sources that aLIGO could detect with current searches. Instead, they suggest an estimate of the number of sources that aLIGO could detect if optimal matched-filtering searches for eccentric sources were to be used. For events with eccentricities greater than 0.1, this rate is ∼0.2 yr^{-1} (pessimistically ∼0.02 yr^{-1}, optimistically ∼0.5 yr^{-1}), while for mergers with eccentricities greater than 0.9, the rate becomes ∼0.2 yr^{-1} (pessimistically ∼0.01 yr^{-1}, optimistically ∼0.4 yr^{-1}). We note also that that the corresponding waveforms of most eccentric GW sources discussed here are characterized by a sequence of bursts of energy emitted near periapsis rather than a continuous waveform. Because of this, matched filtering techniques could be unpractical and a power stacking algorithm might be employed instead (East et al. 2013). The disadvantage is that this will not give an optimal signal-to-noise ratio which might somewhat reduce the detection rates for eccentric inspirals we find.

Table 1 summarizes the main results of our rate computation giving the predicted aLIGO detection rate of binary BH mergers from GCs. This table also gives the corresponding compact binary coalescence rates per GC per Myr. Table 1 gives the rate of LK induced BH mergers (hierarchical triples), and the rate of mergers due to the LK mechanism that have an eccentricity larger than 0.1 at 10 Hz frequency (eccentric inspirals). From our Monte Carlo models we also computed the merger rate of hard escapers that will merge in the galactic field within one Hubble time (ejected binaries) and the rate of mergers occurring *inside* the clusters that are not due to the LK mechanism (in-cluster mergers). These latter include mergers due to binary–single dynamical interactions, as well as those mergers due to binary stellar evolution and single–single captures (see Rodriguez et al. 2015, for details).

In agreement with previous calculations (e.g., O'Leary et al. 2006; Downing et al. 2010) we find that the total event rate is largely dominated by outside cluster mergers. We stress again that the BH mergers due to the LK mechanism will occur inside the GC. Thus, by comparing the rate estimates for triples to the rate of in-cluster mergers due to other processes in Table 1 we can conclude that the detection rate of BH mergers occurring *inside* the cluster is dominated by the rate of LK induced mergers. This is somewhat surprising given that in-cluster mergers that do not occur in triples account for approximately 10% of the total binary BH mergers over 12 Gyr. The low aLIGO event rate we find is a consequence of the fact that the majority of these mergers occur early in the cluster's lifetime, and are relatively low-mass. Since aLIGO is less sensitive to low-mass, high-redshift sources, the rate of detected sources drops. We conclude that mergers induced by LK oscillations in hierarchical triples are likely to be the main contributor to in-cluster GW sources for aLIGO detectors, and represent ∼1% of

[2] "https://dcc.ligo.org/cgi-bin/DocDB/ShowDocument?docid=2974" LIGO Document T0900288-v3.

Table 1
aLIGO Detection and Merger Rates of Coalescing BH Binaries from GCs

Source	Detection Rates (yr^{-1})			Merger Rates (GC^{-1} Myr^{-1})		
	Low	Realistic	High	Low	Realistic	High
Hierarchical triples	0.11	0.47	1.9	1.9×10^{-4}	2.8×10^{-4}	3.3×10^{-4}
Eccentric inspirals	0.021	0.20	0.48	3.4×10^{-5}	5.7×10^{-5}	7.3×10^{-5}
In-cluster mergers	0.011	0.062	0.60	1.9×10^{-4}	2.8×10^{-3}	3.4×10^{-3}
Ejected binaries	10	30	100	0.015	0.023	0.027

Note. In-cluster mergers are defined here as all events occurring inside the GC Monte Carlo Models that are not due to the LK mechanism. As Described in the text, the detection rate for eccentric sources ($e_1[\gtrsim 10\,\mathrm{Hz}] \gtrsim 0.1$) represents the number of inspirals that could be detected with dedicated search strategies.

the anticipated total detection rate of BH binary mergers assembled in GCs.

5. RESULTS: STELLAR TRIPLES

In total, our Monte Carlo models produced 2940 triples in which both components of the inner binary were MS stars (i.e., stellar triples). Following the same procedure adopted above, we made 10 realizations for each triple, taking a random orientation between the two orbits and random orbital phases. We then integrated the triples forward in time using ARCHAIN if the condition (9) (with $D_{\rm diss} = 2[R_0 + R_1]$) was satisfied; the rest of the initial conditions were integrated using the octupole level secular equations of motion based on the double average Hamiltonian (e.g., Michaely & Perets 2014; Naoz & Fabrycky 2014). Each integration was terminated either at $T_{\rm enc}$, or when one of the binary components had passed within its Roche limit.

In many of our simulations the inner binary reaches very high eccentricities, implying a high probability that the stars will cross each other's Roche limit and transfer mass. To account for the possibility of crossing the Roche limit, we check whether the condition $d_{ij} L_{R,ij} < R_i$ (or $a_1(1-e_1)L_{R,ij} < R_i$ in orbit average integrations) was met, with d_{ij} as the instantaneous distance between the two inner binary components and (Eggleton 1983):

$$L_{R,ij} = 0.49 \frac{\left(m_i/m_j\right)^{2/3}}{0.6\left(m_i/m_j\right)^{2/3} + \ln\left(1 + \left(m_i/m_j\right)^{1/3}\right)}. \quad (16)$$

As often done in the literature, we stopped the integration and assumed that the binary had merged if one of the two binary components had passed within its Roche limit (e.g., Naoz & Fabrycky 2014). We found that in 10,327 out of the overall 29,400 triples, 1 of the inner binary components crossed its Roche limit. After accounting for the fact that we have explored a limited range of orbital inclinations, we find an overall probability of $\sim$10% that a stellar triple assembled dynamically in a GC will lead to a mass transfer event and possibly to a stellar merger.

Figure 7 gives the ratio of the triple survival timescale, to the LK timescale plotted as a function of $a_2(1-e_2)/a_1$. Mass-transfer systems are indicated by blue colored symbols. This plot shows that the survival timescale for these systems can be many orders of magnitude larger than the corresponding LK timescale. The ratio $T_{\rm enc}/T_{\rm LK}$ for these systems is also typically larger than that for BH triples (compare to Figure 3), reflecting the different tertiary period distribution of the two populations shown in Figure 1 and the larger binary mass in the case of BH

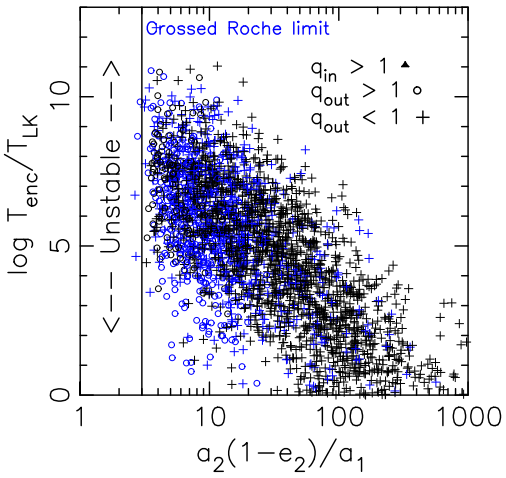

Figure 7. Similar to Figure 3 but for stellar triples. Blue symbols are systems in which one component of the inner binary crossed the Roche limit during the evolution.

components. In Figure 7 we identify those systems for which the orbit average approximation breaks down. In agreement with our previous discussion, most of these systems correspond to compact configurations in which the tertiary comes closer to the inner binary than a separation $a_2(1-e_2)/a_1 \lesssim 100$. We also identify those systems in which in at least 1 of the 10 random realizations one of the inner binary components crossed its Roche limit. Not surprisingly, close outer orbits are more likely to result in a mass transfer event between the inner binary components.

In Figure 8 we consider the distribution of orbital periods. Figures 9 and 10 display respectively the distribution of merger times and mass of the merger remnant for systems that crossed their Roche limit. These distributions were obtained using the weighing technique described in Section 4, i.e., weighing the number of systems for each cluster model by the likelihood of that model to represent a MW-like GC.

In Figure 8 we show the initial and final orbital period distributions of the systems that did not cross the Roche limit, as well as the initial period distributions of the systems that crossed the Roche limit during the evolution. As shown in this figure the peak of the period distribution of the surviving binaries shifts from $\sim$3.2 to $\sim$1 day. This is a consequence of energy loss due to tidal dissipation that the binary experiences during the high eccentricity phases of LK cycles. If during the evolution the timescale associated with precession due to tidal and PN terms becomes shorter than the LK timescale, the eccentricity oscillations due to the interaction with the tertiary are suppressed. In this case, after many LK cycles tidal

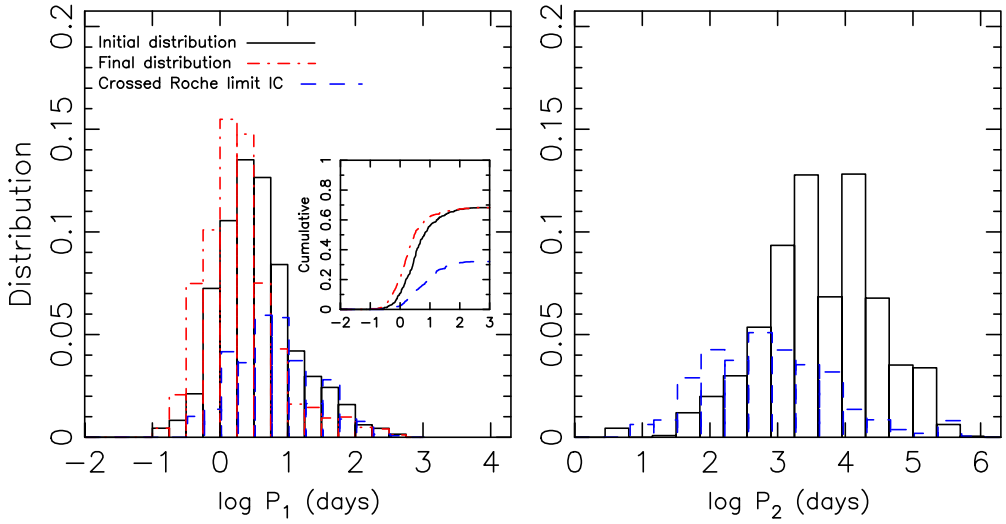

Figure 8. Initial (black lines) and final (dotted–dashed red lines) period distributions for systems in which the inner binary components did not cross the Roche limit during the evolution. Dashed blue lines show the initial period distribution of systems that crossed their Roche limit during the evolution. The distributions are normalized to the total number of systems that were evolved, such that the sum of the integrals of the distribution of not merging systems plus the distribution of merging systems is unity. As explained in the text these distributions should be interpreted as typical distributions for MW-like GCs.

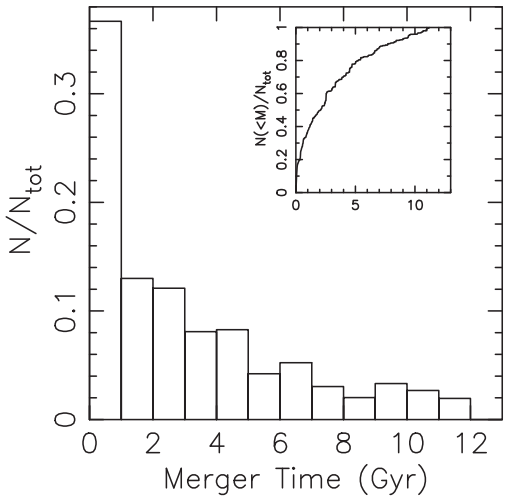

Figure 9. Merger time distribution of stellar binaries produced by the LK mechanism in a MW-like GC. The inset panel shows the corresponding cumulative distribution. The distribution has been normalized to the total number of merging systems.

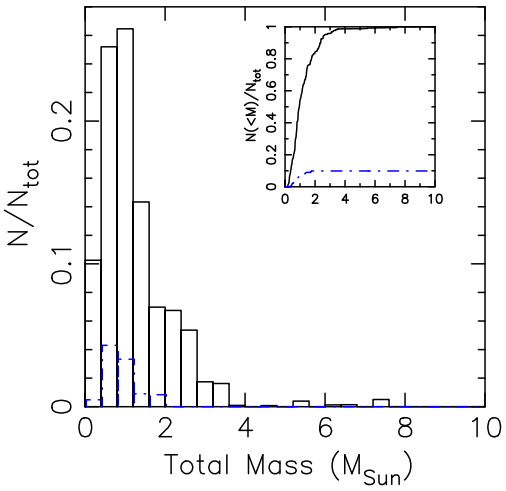

Figure 10. Distribution of the total mass of binaries that crossed the Roche limit during the evolution. Assuming that these binaries will end up merging, such distributions can be interpreted as those corresponding to stellar merger products induced by the LK mechanism in a MW-like GC. The dashed blue lines show the mass distribution of systems that merged in the last 4 Gyr of the cluster evolution. These distributions have been normalized to the total number of merging systems.

dissipation can shrink the binary orbital semimajor axis by a large factor, causing the binary to effectively decouple from the tertiary.

Figure 8 shows that although merging systems are produced at any value of P_1 and P_2, they are more likely to originate from systems with the tightest outer orbits and widest inner binaries. In fact, about half of the systems with $P_2 \lesssim 100$ days or with $P_1 \gtrsim 10$ days led to stellar mergers. Generally in order for the inner binary to attain a quasi-radial orbit such that its components can merge, its eccentricity has to be excited on a timescale much shorter than the typical extra precession timescale (such as tides and relativistic precession). It can be easily shown that the effectiveness of such extra sources of precession decreases with the ratio a_2/a_1 (e.g., Blaes et al. 2002), which is consistent with the fact that mergers are more likely to occur for wide inner binaries and close outer orbits.

The distribution of merger times for stellar binaries is shown in Figure 9. Given that the merger time through LK cycles is generally very short, the number of merging systems at a given time is also a good measure of the number of hierarchical triples that are formed dynamically in the cluster core at that time interval. Figure 9 shows that ∼40% of all stellar mergers occur in the first Gyr of cluster evolution. This is expected given that it is only during these early times that the stars dominate the cluster core where stellar binary–binary encounters can take place at a high rate and lead to the assembly of stellar triples. After ∼1 Gyr of evolution, the BHs have already decayed to the center through dynamical friction becoming the dominant population in the cluster core. As the BHs become dominant, interactions involving stellar binaries become less frequent, naturally reducing the formation rate of triples with

stellar components and favoring the formation of BH triple systems instead.

Finally, Figure 10 displays the total mass distribution of all binaries that underwent Roche-lobe overflow during their evolution. This plot shows that the merging systems have masses up to $\approx 8\ M_{\odot}$, with a peak at about $1\ M_{\odot}$. The most massive mergers, including a few at $\gtrsim 4\ M_{\odot}$, were found to occur only very early in the first few Gyr. As illustrated by the dashed blue lines in Figure 10, no merger with mass larger than $\sim 2\ M_{\odot}$ was found during the last 4 Gyr of cluster evolution. These late mergers have a typical mass of 0.5–1 $M_{\odot}$, as expected since they are about twice the mass of an average MS star of an old single stellar population.

5.1. Formation of Blue Stragglers

BSSs are main sequence stars that appear to be hotter and more luminous than the turn-off point for their parent cluster population. As such they appear to be younger than the rest of the stellar population (e.g., Sandage 1953).

BSSs are created when an MS star is replenished with new supply of hydrogen in its core. Hence, they can remain in the MS longer than expected of an undisturbed star. This can happen through mass transfer in a binary system or via merger/collision with at least one MS star (see Perets 2015 for a recent review). Perets & Fabrycky (2009) suggested that triples might be a natural progenitor for BSSs, as the high eccentricities attained during LK cycles can lead to tidal interaction, mass loss or even a merger of the inner binary components. Although dynamically formed triples are expected to form quite efficiently in GCs, their long term dynamical evolution in GCs has not been yet investigated. Hence, until now their role in BSS formation remains largely unconstrained. In what follows we use our Monte Carlo models, coupled with the results of the three-body integrations, to determine the relative contribution of triples to BSSs in GCs.

Besides BSSs possibly produced by the LK mechanism, we also computed the number of BSSs due to binary-mediated interactions, i.e., mass transfer and physical collisions. We computed the number of BSSs at the observation time of ~ 12 Gyr in each model in the following way. We first estimate the MS turn-off mass ($m_{\rm TO}$) given the metallicity and age of the model cluster in question. From the snapshot containing all stars we then extract those that are still on their MS and has mass $\geqslant 1.05 \times m_{\rm TO}$. In theory, any MS stars with mass above $m_{\rm TO}$ are BSSs, however, observationally, it is hard to distinguish BSSs from the MS if their masses are not high enough compared to $m_{\rm TO}$. This simple mass-based prescription results in very good agreement between observationally extracted BSS numbers, their stellar properties, and known correlations between BSS and observable properties of the cluster (e.g., Leigh et al. 2011; Chatterjee et al. 2013; Sills et al. 2013, for more details).

Figure 11 shows the relative importance of BSS production via traditional binary-mediated channels and triples. Since the triples were not followed in the Monte Carlo models, BSSs created via LK cycles leading to mass transfer or merger between the inner binary can only be calculated for each triple produced in the models. For these cases we cannot directly consider the subsequent stellar evolution of the BSSs. For example, whether followed by a merger the BSS created via a triple-mediated channel later evolves off of the MS before the observation time of ~ 12 Gyr, cannot be directly determined in this setup. Indeed, in detailed models it had been found that BSSs can live in the MS for several billion years after formation. It is also expected that the median age since formation for the observed BSSs can vary depending on the dominant formation channel for the BSSs in a real cluster (e.g., Chatterjee et al. 2013). The real age since formation for BSSs, even in these detailed models, might not be accurate, since the residual rejuvenated lifetime for a real BSS depends intricately on the details of the degree of H-mixing in the core which in turn depends on the details of the interaction that produced it (e.g., Sills et al. 2001; Lombardi et al. 2002; Chen & Han 2009; Chatterjee et al. 2013). Instead, we report two quantities for the triple-mediated BSSs: (1) The total number of mergers or Roche-filling architectures created from dynamically formed triples during the full evolution of the model clusters, and (2) the same, but for binaries with a total mass $\geqslant 1.05 \times m_{\rm TO}$ and created only within the last 4 Gyr, an estimated upper limit of today's observed BSSs in typical Galactic GCs (Chatterjee et al. 2013). We find that the relative importance of triple-mediated channels is low compared to binary-mediated channels for BSS production. The importance of triple-mediated channels is $\lesssim 10\%$ for the cluster models considered in this work.

There is a lot of interest in BSSs found in binaries. Often these systems are thought to be produced via stable mass transfer in a binary where the donor stays bound to the accretor. On the other hand, these may also be produced via triple-mediated channels where the inner binary merges and the outer binary is hard and remains unbroken (e.g., Fabrycky & Tremaine 2007; Perets & Fabrycky 2009; Perets 2015; Gosnell et al. 2015). We find that the contribution from triple-mediated channels for binary BSSs is also small being $\lesssim 10\%$ of the number of mergers due to binary-mediated processes. In addition, we find that the binary BSSs coming via binary-mediated channels are *not* simply coming from mass transfer in a binary. Collisionally produced BSSs can frequently acquire a binary companion via binary–single scattering encounters. Since BSSs are more massive compared to typical cluster stars at late ages, initially single BSSs, created earlier via a merger or physical collision, can frequently acquire a binary companion via exchange with another normal star in a binary through binary–single interactions. This is consistent with earlier work that investigated the detailed history and branching ratios of various binary-mediated formation channels for BSSs produced in similar models (Chatterjee et al. 2013).

6. DISCUSSION

6.1. Implications for GW Detectors and Comparison to other Sources of Eccentric GW Inspirals

The first GW signal from a compact object binary is likely to be detected in the coming years by Advanced ground-based laser interferometers (Aasi et al. 2015; Acernese et al. 2015). Most GW searches adopt matched filtering techniques in which the detector signal is cross-correlated with banks of theoretical gravitational waveforms to enable detection of the weak signals. Mainly due to computational limitation, such banks of theoretical waveforms are exclusively composed of circular binaries. However, there are many reasons to extend the searches to also include eccentric inspirals. First, there have been recent developments of dedicated techniques that will potentially enable the detection of eccentric sources (Huerta

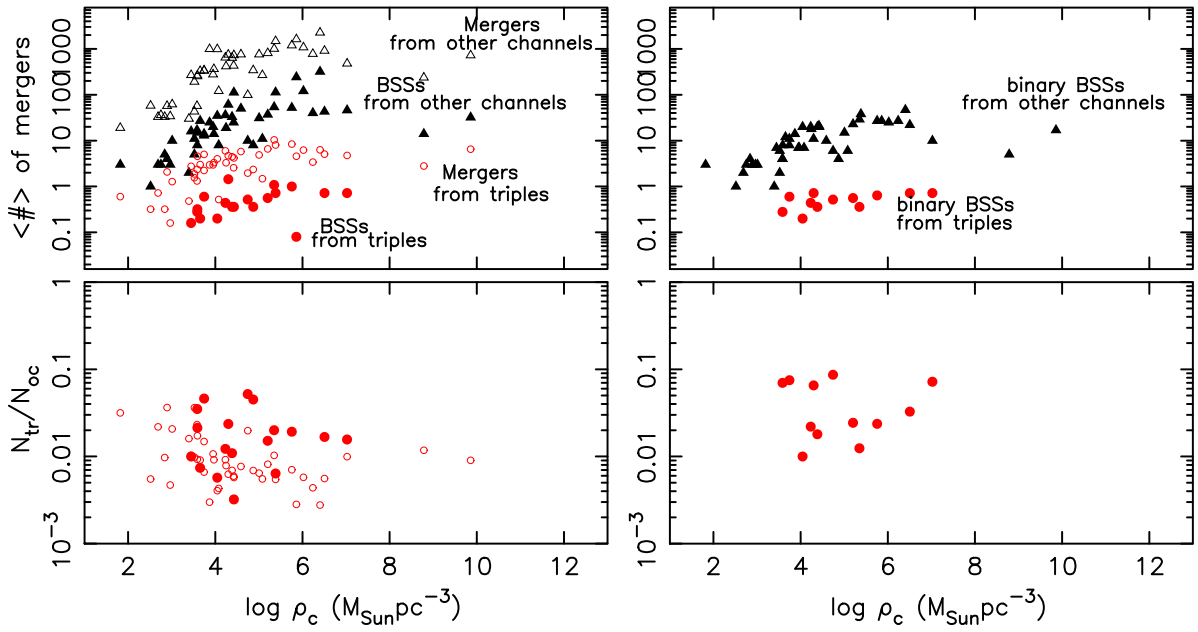

Figure 11. Contribution of triples to the population of BSSs (left panels) and binary BSSs (right panels) in GCs. In the upper left panels, filled and open circles represent, respectively, the total number of BSS candidates and stellar mergers formed in triples. The filled and open triangles show, respectively, the total number of BSSs and stellar mergers in our cluster models that were not produced in hierarchical triples. In the right panels filled circles represent BSSs from hard triples with an MS star tertiary. The latter are the systems that will survive as binaries up to the present epoch and could be observed as binary BSSs. In the lower panels the filled circles give the ratio of the number of (binary) BSSs formed in triples (N_{tr}) to the number of BSSs due to other channels (N_{oc}). The open circles give the number of stellar mergers from tripleS divided by the total number of stellar mergers from binary mediated channels. These quantities are all plotted against the central density of the model at 12 Gyr. Note that a few clusters are in a state of core-collapse at this time, being characterized by very high central densities ($\rho_c \gtrsim 10^8\,M_\odot\,\mathrm{pc}^{-3}$).

et al. 2014; Tai et al. 2014; Akcay et al. 2015; Coughlin et al. 2015). Second, eccentric inspirals produce a GW signal which is distinct from that of circularly inspiraling binaries, and provides more insights on the strong-field dynamics (Loutrel et al. 2014; Akcay et al. 2015; Le Tiec 2015). Finally, as discussed below, there are several dynamical mechanisms that can lead to the formation of eccentric GW sources. The detection of such eccentric sources could provide important information about properties (e.g., triple/binary fraction, central densities) of compact object populations in GCs and galactic nuclei that will be otherwise inaccessible.

Several mechanisms have been proposed for the formation of eccentrically inspiraling compact binaries for high frequency GW detectors. These include: (i) BH–BH scattering in steep density cusps around massive black holes (MBHs; O'Leary et al. 2009; Kocsis & Levin 2012), (ii) binary–single compact object encounters in star clusters (Samsing et al. 2014) and (iii) LK resonance in hierarchical triple systems forming in the dense stellar environment of galactic nuclei (Antonini & Perets 2012) or stellar clusters (e.g., Wen 2003, this paper). In this section we discuss the rate for eccentric compact binary coalescences that could be detectable by aLIGO. With the caution that rate estimates remain subject to significant uncertainties, we find that BH binary mergers from hierarchical triples in GCs are likely to dominate the production of eccentric inspirals that could be detectable by Advanced ground-based laser interferometers.

Single–single captures. In galactic nuclei with MBHs, nuclear relaxation times can often be less than a Hubble time, and can result in the formation of steep density cusps of stellar-mass BHs as a consequence of mass segregation against the lower mass stars (e.g., Hopman & Alexander 2006). O'Leary et al. (2009) proposed that in such dense population environments BH binaries can efficiently form out of GW emission during BH–BH encounters. After forming, these BH binaries rapidly inspiral and merge within a few hours. O'Leary et al. (2009) found that ∼90% of these coalescing binaries will have an eccentricity larger than 0.9 inside the aLIGO frequency band. The predicted rate for eccentric capture of 10 $M_\odot$ BH–BH encounters is $\sim 0.01\,\mathrm{yr}^{-1}\,\mathrm{Gpc}^{-3}$ (Tsang 2013).

Table 1 of O'Leary et al. (2009) presents the merger rate per MW-like galaxy and for different cusp models. The plausible pessimistic, likely, and optimistic rates can be taken from models Aβ3, E-2, and F-1 of their Table 1. The most optimistic scenario, given by model F-1, produces a merger rate of $1.5 \times 10^{-2}\,\mathrm{Myr}^{-1}$. The realistic scenario, identified here with model E-2, predicts $1.3 \times 10^{-3}\,\mathrm{Myr}^{-1}$. The pessimistic scenario, given by model Aβ3, produces $2 \times 10^{-4}\,\mathrm{Myr}^{-1}$. We can compare these merger rates with those corresponding to eccentric inspirals from GCs. After multiplying the merger rates in our Table 1 by a factor 200 (roughly the number of GCs in the MW; Harris et al. 2014), we see that the realistic merger rate for the O'Leary et al. (2009) scenario appears to be about one order of magnitude smaller than the realistic merger rate of eccentric inspirals from GCs.

Hong & Lee (2015) carried out *N*-body simulations of star clusters around MBHs to study the formation of BH binaries in nuclear clusters and to put constraints on the aLIGO detection rates for the O'Leary et al. (2009) model. Hong & Lee (2015) derived an aLIGO expected detection rate of $0.02\text{–}14\,\mathrm{yr}^{-1}$ depending on the maximum horizon distance assumed and the mass ratio of MBH to the surrounding cluster. As also noted by Hong & Lee (2015), these rates are likely to be an overestimate of the real event rate from BH–BH captures. They were in fact obtained by assuming that the mass fraction of BHs is 44% of the total cluster mass, which is only reasonable within about

one-tenth of the MBH influence radius of a mass-segregated nuclear cluster (Hopman & Alexander 2006). Given that most of the captures were found to occur near the half-mass radius of the nuclear cluster, where mass segregation will not significantly alter the initial number fraction of different mass species (Antonini 2014), a more reasonable choice would be to simply adopt a BH mass fraction similar to that expected on the basis of the initial mass function of the underlining population. For example, in the Galactic center there is evidence for a standard Kroupa-like initial mass function (Löckmann et al. 2010) which will result in 1% only of the total mass in BHs (Hopman & Alexander 2006). Using this standard choice for the initial mass function and adopting the same quadratic scaling on the BH mass fraction of Hong & Lee (2015) will cause the estimated detection rates to drop by approximately three orders of magnitude.

*Binary–single encounters.*The in-cluster detection rate reported in Table 1 includes BH mergers due to single–binary interactions. Assuming that 1% of these mergers will have a finite eccentricity within the aLIGO band (Samsing et al. 2014) results in a negligible contribution of binary–single encounters to the population of eccentric inspirals when compared to the triple channel.

Samsing et al. (2014) studied binary–single stellar scattering occurring in dense star clusters as a source of eccentric NS–NS inspirals for aLIGO. During the chaotic gravitational interaction between the three bodies, a pair of compact objects can be driven to very high eccentricities such that they can inspiral through GW radiation and merge. Samsing et al. (2014) argued that 1% of dynamically assembled NS–NS merging binaries will have a substantial eccentricity at $\gtrsim$10 Hz frequency. Samsing et al. (2014) also give a simple order of magnitude estimate of the merger rate for dynamical NS–NS star eccentric inspirals assembled in GCs of 0.7 $\mathrm{yr}^{-1}\,\mathrm{Gpc}^{-3}$.

To compare to the event rate we found for eccentric LK induced mergers in GCs we recompute the Samsing et al. (2014) rates by rescaling with the different GC number density used in Section 4.1. Samsing et al. (2014) calculate the rate of eccentric binaries in the aLIGO band adopting $\rho_{\rm GC} = 10\ \mathrm{GC\ Mpc}^{-3}$. Taking $\rho_{\rm GC} = 0.77\ \mathrm{GC\ Mpc}^{-3}$ instead, assuming that aLIGO will see NS–NS mergers up to a sky-averaged distance of 400 Mpc (Abadie et al. 2010), and optimistically assuming that mergers are distributed uniformly over the lifetime of the globulars (as opposed to happening early on in the lifetime of the cluster), this translates into a possible aLIGO detection rate for NS–NS eccentric inspirals of $\sim$0.02 yr^{-1}.

We note that Coughlin et al. (2015) give in their Table II the potential detection rates for the model of Samsing et al. (2014). These rates appear to be larger by one order of magnitude than our rate estimate above. We believe, however, that the rates computed by Coughlin et al. (2015) were mistakenly enhanced due to a misinterpretation of Samsing et al. (2014) results. Samsing et al. (2014) found that about "1% of *dynamically* assembled non-eccentric binaries" will have a finite eccentricity at 10 Hz. Coughlin et al. (2015) computed the rates in their Table II as the 1% of the *total* compact merger rate given in Table V of Abadie et al. (2010) which corresponds, however, to predictions for *field* mergers. In order to correct for this we have to multiply the rates in Table II of Coughlin et al. (2015) by the expected fraction of all compact object mergers that are dynamically assembled in star clusters. Taking this fraction to be 10% of all NS–NS mergers (Grindlay et al. 2006; Samsing et al. 2014), and assuming that 1% of these are eccentric inspirals results in $4 \times 10^{-3}\,\mathrm{yr}^{-1}$, $0.04\,\mathrm{yr}^{-1}$, and $0.4\,\mathrm{yr}^{-1}$ for the low, realistic, and high detection rates for binary NSs. These estimates appear to be in good agreement with the rate of $\sim$0.02 yr^{-1} we previously computed.

Although very simplified, the simple calculations presented above show that, even when assuming a uniform rate of mergers, the rate of eccentric NS binaries in the aLIGO frequency band is likely 1–2 orders of magnitude smaller than the realistic estimates for eccentric BH binaries forming through the LK mechanism in GCs.

MBH mediated compact-object mergers in galactic nuclei. Antonini & Perets (2012) studied the evolution of compact object binaries orbiting a MBH. Near the galactic center, where orbits are nearly Keplerian, binaries form a triple system with the MBH in which the latter represents the outer perturber of the triple. The MBH can subsequently drive the inner binary orbit into high eccentricities through LK resonance, at which point the compact object binary can efficiently coalesce through GW emission. Antonini & Perets (2012) found that $\approx$10% of such coalescing binaries will evolve through the dynamical non-secular evolution similar to that described in Section 2, leading to finite eccentricity sources in the aLIGO sensitivity window.

Antonini & Perets (2012) estimated a BH–BH eccentric inspiral rate for a MW-like galaxy between 10^{-5} and $10^{-2}\,\mathrm{Myr}^{-1}$. These rates are somewhat comparable to the rates for BH–BH mergers due to GW captures derived by O'Leary et al. (2009); however, they are still smaller than the rates for eccentric inspirals assembled in GCs for a MW-like galaxy given in Table 1, and even under the most optimistic assumptions, they are still only 3% of the realistic and 0.01 % of the high/optimistic rate in Abadie et al. (2010).

Given the realistic BH–BH detection rate with aLIGO of $\sim$20 yr^{-1} (Abadie et al. 2010), the predicted overall rate of eccentric compact binary coalescence in the aLIGO band induced by MBH mediated LK cycles in galactic nuclei is $\sim$0.02 yr^{-1} (Coughlin et al. 2015). We conclude that the overall contribution of eccentric GW sources from galactic nuclei is likely negligible compared to the rate of eccentric mergers arising from hierarchical triples in GCs.

6.2. Implications for Blue Straggler Formation

The BSSs observed abundantly in all clusters have long been recognized as a way of identifying important stages in the host cluster's history. However, interpretation of observed trends between the BSS number and cluster properties is dependent on the relative importance of the various BSS formation channels in these clusters. Especially, there has been a long history of carefully considering correlations between the number of BSSs produced in a cluster and several dynamically important observed cluster properties, including the total mass, total number of binaries, and the central collision/interaction rate, and what they mean (Piotto et al. 2004; Leigh et al. 2007; Knigge et al. 2009; Chatterjee et al. 2013). Although, it has been pointed out that formation of BSSs from triple-mediated interactions may be important, at least in open clusters (Leigh & Sills 2011), this has never been self-consistently investigated in realistic and evolving cluster models (Perets 2015). As part of this study we have considered the evolution of triples created dynamically in the cluster models and analyzed them as

potential BSS progenitors. Upon comparison of the estimated numbers of the BSSs resulting from triple-mediated formation channels to those formed via binary-mediated channels (mass transfer and physical collisions due to binary-mediated interactions), we find that, at least for GC-like densities, contribution from triple-mediated channels is quite low.

For the triple-mediated BSSs, we did not consider whether upon formation the rejuvenated MS star will remain in the region expected of BSSs in a color-magnitude diagram. The rejuvenated lifetime of BSSs is model dependent and hard to estimate. For the binary-mediated BSSs we assume full-mixing of hydrogen. In the case of triple-mediated BSSs, we simply compare the total number of BSSs created throughout the lifetime of the GC and that formed within the last 4 Gyr and with mass $\geqslant 1.05 \times m_{\rm TO}$. Thus, the actual contribution from triple-mediated interaction may be even lower if many of these BSSs evolve off of their rejuvenated MS before the observation time of $\sim$12 Gyr.

We note that above we have not considered BSS formation through binary evolution in short period binaries affected by the LK mechanism coupled with tidal friction. The shrinkage of the inner binary semimajor axis as well as the high eccentricities induced via the LK mechanism, combined with an expansion in the size of each inner binary star, could lead to coalescing/strongly interacting post-MS binaries. In order to address the importance of this alternative channel we determined whether the stars would undergo mass transfer by requiring their periapsis distance to be smaller than the Roche limit computed through Equation (16) and setting the stellar radius of the most massive component equal to that evaluated at the tip of the red giant branch (Hurley et al. 2000). The periapsis distance was evaluated using the orbital parameters at the end of the three-body integrations. We only considered stars with mass $\gtrsim 0.7\ M_{\odot}$ so that their MS lifetime was shorter than the host GC age. Also, we did not consider systems that will have undergone mass transfer on the red giant branch even without the help of LK cycles and tidal dissipation. We found that only 694 of the total 19,073 binaries that did not merge during the MS would merge on the red giant branch through a combination of LK cycles, tidal friction, and the expansion of the stellar radius caused by stellar evolution. This calculation suggests that the number of BSSs formed through a combination of LK dynamics and stellar evolution in our models is negligible.

Finally, note that we did not consider primordial triples that could somewhat increase the number of mergers from stellar triples shown in Figure 11. However, we think that mergers occurring in primordial triples will have a negligible contribution to BSSs compared to mergers from dynamically assembled triples. In fact, due to the high stellar densities of GCs the outer binaries in primordial triples are likely to be involved in several dynamical encounters which will lead to their disruption in the first few Gyr of cluster evolution. The majority of triples in the catalog of Riddle et al. (2015) have outer period $P_2 \gtrsim 10^4$ days, which according to Equation (12) corresponds to a typical survival time $T_{\rm enc} \lesssim 10^9$ years within the core of a GC and $T_{\rm enc} \lesssim 10^{10}$ in the cluster outskirts (see also Figure 2 of Perets & Fabrycky 2009). Moreover, given the old age of GCs stellar merger products that occurred in primordial triples would have already evolved off the main sequence, so that only dynamically formed triples could then produce BSSs at later stages of cluster evolution.

7. SUMMARY

In this paper we studied the long-term evolution of dynamically assembled triples in GCs. The initial conditions for the triples were obtained directly from detailed Monte Carlo models of the clusters. These systems consisted mostly of triples containing an inner stellar binary and triples containing a pair of BHs. The triple initial conditions were integrated forward in time using a high accuracy three-body integrator which incorporates relativistic corrections and tidal terms to the equations of motion. The direct integrations allowed us, for the first time, to put constraints on the contribution of the LK mechanism to the population of coalescing BH binaries and BSSs in GCs. The main results of our study are briefly summarized below.

(1) We find that for the majority of dynamically assembled triple systems in GCs, the timescale for changes of angular momentum during the high eccentricity phase of a LK cycle becomes shorter than the orbital timescales. We conclude that the standard orbit average equations of motion, often employed in previous studies, cannot accurately describe the evolution of such triples.

(2) BH triples assembled dynamically in GCs often evolve such that the inner binary angular momentum changes on timescales of the order of or shorter than the inner binary orbital period (see Figure 2). This can lead to the formation of eccentric GW sources in the frequency band of aLIGO detectors (see Figure 3).

(3) We estimated a realistic aLIGO detection rate of BH binary mergers due to the LK mechanism of $\sim 1\ {\rm yr}^{-1}$. We also compared this rate to that for BH mergers due to other processes (see Table 1). We find that mergers induced by LK oscillations are likely to be the main contributor to in-cluster GW sources for aLIGO detectors, and represent $\sim$1% of the total detection rate of BH binary mergers assembled in GCs.

(4) About 20% of all LK mechanism-induced BH mergers in GCs will have an eccentricity larger than $\sim$0.1 at 10 Hz frequency, such that eccentric waveform templates and/or dedicated search strategies will be needed for their efficient detection (see Figure 4). Most of these eccentric sources will have an extremely large eccentricity $(1 - e \lesssim 10^{-4})$ at the moment they first enter the aLIGO frequency band. Assuming perfect waveform templates, we find a possible detection rate for eccentric mergers as large as a few events a year with aLIGO. We also show that the triple channel is likely the dominant formation mechanism for the production of eccentric inspirals that will be potentially detectable by aLIGO.

(5) In the case of triples containing a stellar binary, the inner binary angular momentum often changes on timescales shorter than the tertiary orbital period, but rarely shorter than the *inner* binary orbital period. This implies that "clean" collisions between two stars, in which all passages prior to the collision are greater than the tidal dissipation scale, are rare (see Figure 1).

(6) We estimated the number of BSSs expected to form through mergers induced by the LK mechanism as well as those formed through other processes, including binary stellar evolution, binary–single scattering and direct collisions (see Figure 11). We find that the contribution of LK-induced mergers to the population of BSS populations in GCs is typically $\lesssim$10% of the total. Even in clusters with relatively low central densities ($\sim 10^{2-3}\ M_{\odot}\ {\rm pc}^{-3}$) only up to $\sim$10% of

BSS binaries could have formed in dynamically assembled triples.

We are grateful to S. Mikkola, who wrote the ARCHAIN algorithm and who generously assisted us in using it. During the course of this work, we have benefited from conversations with several colleagues, including Cole Miller and Hagai Perets. We thank the referee for useful comments that helped to improve this paper. F.A. acknowledges support from a CIERA postdoctoral fellowship at Northwestern University. This work was supported by NASA ATP Grant NNX14AP92G and NSF Grant AST1312945. S.C. also acknowledges support from NASA through a grant from the Space Telescope Science Institute, which is operated by the Association of Universities for Research in Astronomy, Inc., under NASA contract NAS5-26555; the grant identifying number is HST-AR-12829.004-A. V.K. and F.A.R. also acknowledge support from NSF Grant PHY-1066293 through the Aspen Center for Physics.

REFERENCES

Aasi, J., Abadie, J., Abbott, B. P., et al. 2015, CQGra, 32, 115012
Abadie, J., Abbott, B. P., Abbott, R., et al. 2010, CQGra, 27, 173001
Acernese, F., Agathos, M., Agatsuma, K., et al. 2015, CQGra, 32, 024001
Akcay, S., Le Tiec, A., Barack, L., Sago, N., & Warburton, N. 2015, PhRvD, 91, 124014
Antognini, J. M., Shappee, B. J., Thompson, T. A., & Amaro-Seoane, P. 2014, MNRAS, 439, 1079
Antonini, F. 2014, ApJ, 794, 106
Antonini, F., Faber, J., Gualandris, A., & Merritt, D. 2010, ApJ, 713, 90
Antonini, F., Murray, N., & Mikkola, S. 2014, ApJ, 781, 45
Antonini, F., & Perets, H. B. 2012, ApJ, 757, 27
Arca-Sedda, M. 2016, MNRAS, 455, 35
Binney, J., & Tremaine, S. 1987, Galactic Dynamics (Princeton, NJ: Princeton Univ. Press), 747
Blaes, O., Lee, M. H., & Socrates, A. 2002, ApJ, 578, 775
Bode, J. N., & Wegg, C. 2014, MNRAS, 438, 573
Brown, D. A., & Zimmerman, P. J. 2010, PhRvD, 81, 024007
Chatterjee, S., Fregeau, J. M., Umbreit, S., & Rasio, F. A. 2010, ApJ, 719, 915
Chatterjee, S., Rasio, F. A., Sills, A., & Glebbeek, E. 2013, ApJ, 777, 106
Chen, X., & Han, Z. 2009, MNRAS, 395, 1822
Coughlin, M., Meyers, P., Thrane, E., Luo, J., & Christensen, N. 2015, PhRvD, 91, 063004
Downing, J. M. B., Benacquista, M. J., Giersz, M., & Spurzem, R. 2010, MNRAS, 407, 1946
East, W. E., McWilliams, S. T., Levin, J., & Pretorius, F. 2013, PhRvD, 87, 043004
Eggleton, P. P. 1983, ApJ, 268, 368
Fabrycky, D., & Tremaine, S. 2007, ApJ, 669, 1298
Ford, E. B., Kozinsky, B., & Rasio, F. A. 2004, ApJ, 605, 966
Geller, A. M., Hurley, J. R., & Mathieu, R. D. 2013, AJ, 145, 8
Gosnell, N. M., Mathieu, R. D., Geller, A. M., et al. 2015, arXiv:1510.04290
Grindlay, J., Portegies Zwart, S., & McMillan, S. 2006, NatPh, 2, 116
Hamers, A. S., Perets, H. B., Antonini, F., & Portegies Zwart, S. F. 2015, MNRAS, 449, 4221
Hamers, A. S., Pols, O. R., Claeys, J. S. W., & Nelemans, G. 2013, MNRAS, 430, 2262
Harris, W. E., Morningstar, W., Gnedin, O. Y., et al. 2014, ApJ, 797, 128
Hénon, M. H. 1971, Ap&SS, 14, 151
Hogg, D. W. 1999, arXiv:astro-ph/9905116
Holman, M., Touma, J., & Tremaine, S. 1997, Natur, 386, 254
Hong, J., & Lee, H. M. 2015, MNRAS, 448, 754
Hopman, C., & Alexander, T. 2006, ApJL, 645, L133
Huerta, E. A., & Brown, D. A. 2013, PhRvD, 87, 127501
Huerta, E. A., Kumar, P., McWilliams, S. T., O'Shaughnessy, R., & Yunes, N. 2014, PhRvD, 90, 084016
Hurley, J. R., Pols, O. R., & Tout, C. A. 2000, MNRAS, 315, 543
Hut, P. 1981, A&A, 99, 126
Ivanova, N., Heinke, C. O., Rasio, F. A., Belczynski, K., & Fregeau, J. M. 2008, MNRAS, 386, 553
Katz, B., & Dong, S. 2012, arXiv:1211.4584
Knigge, C., Leigh, N., & Sills, A. 2009, Natur, 457, 288
Kocsis, B., & Levin, J. 2012, PhRvD, 85, 123005
Kozai, Y. 1962, AJ, 67, 591
Leigh, N., & Sills, A. 2011, MNRAS, 410, 2370
Leigh, N., Sills, A., & Knigge, C. 2007, ApJ, 661, 210
Leigh, N., Sills, A., & Knigge, C. 2011, MNRAS, 416, 1410
Le Tiec, A. 2015, arXiv:1506.05648
Lidov, M. L. 1961, Iskusstvennye Sputniki Zemli, 8, 5 English translation in Lidov, M. L. 1962, P&SS, 9, 719
Lidov, M. L., & Ziglin, S. L. 1976, CeMec, 13, 471
Löckmann, U., Baumgardt, H., & Kroupa, P. 2010, MNRAS, 402, 519
Lombardi, J. C., Jr., Warren, J. S., Rasio, F. A., Sills, A., & Warren, A. R. 2002, ApJ, 568, 939
Loutrel, N., Yunes, N., & Pretorius, F. 2014, PhRvD, 90, 104010
Mardling, R. A., & Aarseth, S. J. 2001, MNRAS, 321, 398
Merritt, D. 2013, in Dynamics and Evolution of Galactic Nuclei, ed. D. Merritt (Princeton, NJ: Princeton Univ. Press), 544
Michaely, E., & Perets, H. B. 2014, ApJ, 794, 122
Mikkola, S., & Merritt, D. 2006, MNRAS, 372, 219
Mikkola, S., & Merritt, D. 2008, AJ, 135, 2398
Miller, M. C., & Hamilton, D. P. 2002, ApJ, 576, 894
Morscher, M., Pattabiraman, B., Rodriguez, C., Rasio, F. A., & Umbreit, S. 2015, ApJ, 800, 9
Naoz, S., & Fabrycky, D. C. 2014, ApJ, 793, 137
Naoz, S., Farr, W. M., Lithwick, Y., Rasio, F. A., & Teyssandier, J. 2011, Natur, 473, 187
Naoz, S., Farr, W. M., Lithwick, Y., Rasio, F. A., & Teyssandier, J. 2013, MNRAS, 431, 2155
O'Leary, R. M., Kocsis, B., & Loeb, A. 2009, MNRAS, 395, 2127
O'Leary, R. M., Rasio, F. A., Fregeau, J. M., Ivanova, N., & O'Shaughnessy, R. 2006, ApJ, 637, 937
Pattabiraman, B., Umbreit, S., Liao, W.-k., et al. 2013, ApJS, 204, 15
Perets, H. B. 2015, Ecology of Blue Straggler StarsAstrophysics and Space Science Library, Vol. 413 (Berlin Heidelberg: Springer)
Perets, H. B., & Fabrycky, D. C. 2009, ApJ, 697, 1048
Piotto, G., De Angeli, F., King, I. R., et al. 2004, ApJL, 604, L109
Planck Collaboration Ade, P. A. R., Aghanim, N., et al. 2015, arXiv:1502.01589
Prodan, S., Antonini, F., & Perets, H. B. 2015, ApJ, 799, 118
Rasio, F. A., McMillan, S., & Hut, P. 1995, ApJL, 438, L33
Riddle, R. L., Tokovinin, A., Mason, B. D., et al. 2015, ApJ, 799, 4
Rodriguez, C. L., Morscher, M., Pattabiraman, B., et al. 2015, PhRvL, 115, 051101
Samsing, J., MacLeod, M., & Ramirez-Ruiz, E. 2014, ApJ, 784, 71
Sandage, A. R. 1953, AJ, 58, 61
Santamaría, L., Ohme, F., Ajith, P., et al. 2010, PhRvD, 82, 064016
Seto, N. 2013, PhRvL, 111, 061106
Sigurdsson, S., & Hernquist, L. 1993, Natur, 364, 423
Sills, A., Faber, J. A., Lombardi, J. C., Jr., Rasio, F. A., & Warren, A. R. 2001, ApJ, 548, 323
Sills, A., Glebbeek, E., Chatterjee, S., & Rasio, F. A. 2013, ApJ, 777, 105
Tai, K. S., McWilliams, S. T., & Pretorius, F. 2014, PhRvD, 90, 103001
Thompson, T. A. 2011, ApJ, 741, 82
Tsang, D. 2013, ApJ, 777, 103
Wen, L. 2003, ApJ, 598, 419